Human Molecular Genetics, 2004, Vol. 13, No. 15 ***1535–1549***
doi:10.1093/hmg/ddh167
Advance Access published on June 2, 2004

The intranuclear localization and function of YT521-B is regulated by tyrosine phosphorylation

Ilona Rafalska[1,†], Zhaiyi Zhang[1,†], Natalya Benderska[1], Horst Wolff[3], Annette M. Hartmann[2], Ruth Brack-Werner[3] and Stefan Stamm[1,*]

[1]University of Erlangen, Institute for Biochemistry, Fahrstraße 17, 91054 Erlangen, Germany, [2]Molecular Neurobiology, Department of Psychiatry, Ludwig-Maximilian-University, Nussbaumstr. 7, D-80336 Munich, Germany and [3]Institute for Molecular Virology, GSF-Forschungszentrum für Umwelt und Gesundheit, Ingolstaedter Landstr. 1, D-85764 Neuherberg, Germany

Received February 2, 2004; Revised April 1, 2004; Accepted May 18, 2004

YT521-B is a ubiquitously expressed nuclear protein that changes alternative splice site usage in a concentration dependent manner. YT521-B is located in a dynamic nuclear compartment, the YT body. We show that YT521-B is tyrosine phosphorylated by c-Abl in the nucleus. The protein shuttles between nucleus and cytosol, where it can be phosphorylated by c-Src or p59^{fyn}. Tyrosine phosphorylation causes dispersion of YT521-B from YT bodies to the nucleoplasm. Whereas YT bodies are soluble in non-denaturing buffers, the phosphorylated, dispersed form is non-soluble. Non-phosphorylated YT521-B changes alternative splice site selection of the IL-4 receptor, CD44 and SRp20, but phosphorylation of c-Abl minimizes this concentration dependent effect. We propose that tyrosine phosphorylation causes sequestration of YT521-B in an insoluble nuclear form, which abolishes the ability of YT521-B to change alternative splice sites.

INTRODUCTION

The eukaryotic nucleus contains a large number of specialized domains, such as nucleoli, speckles, Cajal bodies, PML bodies, Gems, SAM68 nuclear bodies and YT bodies (1). Analysis of living cells has revealed that most of these structures are dynamic and often exchange proteins. For example, phosphorylation of pre-mRNA splicing factors causes their release into the nucleoplasm (2). Speckles are dynamic structures (3) and often associate with sites of active transcription (4). In this and other cases, the nuclear structure reflects the function and vice versa (5).

YT521-B is a ubiquitously expressed nuclear protein that was discovered through the association of its glutamic-acid/arginine-rich carboxy domain with splicing factors (6,7). YT521-B defines a novel compartment in the nucleus, the YT body. YT bodies contain sites of active transcription and are in close proximity to speckles and SAM68 nuclear bodies, which contain proteins interacting with YT521-B. YT bodies are dynamic structures that disappear during mitosis and are most pronounced in G1. When all three RNA polymerases are blocked by high concentrations of actinomycin D, YT bodies disperse throughout the nucleoplasm and accumulate in an unsoluble nuclear fraction, which distinguishes them from other nuclear subcompartments. The interaction of YT521-B with other nuclear proteins, such as SAM68 is regulated by tyrosine phosphorylation emanating from src kinases (7).

YT521-B can change splice site selection *in vivo* in a concentration dependent manner (7), either by sequestering splicing factors via protein–protein interaction or by directly binding to nucleic acids via its YTH domain (8). The sequencing of the human genome has demonstrated that humans contain only about 25 000 genes, which is far less than previously expected. Therefore, the generation of protein isoforms through regulated alternative splicing is an important step in the gene expression of complex organisms. The majority of human genes are alternatively spliced. Estimates of the frequency of alternative splicing range between 47% based on EST comparisons and 74% based on exon junction microarrays (9,10). The exact mechanism leading to splice site selection is not fully understood (11). It appears that splice site selection occurs concomitant with transcription (12) by formation of a protein–RNA network of regulatory factors binding both to highly degenerate sequences on the pre-mRNA and to other regulatory factors. This protein

*To whom correspondence should be addressed. Tel: +49 91318524622; Fax: +49 91318524605; Email: stefan@stamms-lab.net
†The authors wish it to be known that, in their opinion, the first two authors should be regarded as joint First Authors.

complex brings splice sites in close vicinity which allows their recognition by the spliceosome (11,13,14). Splice site recognition is a dynamic process, requiring constant building and release of individually weak molecular interactions. As a consequence, splice site selection is achieved by combinatorial control of protein concentration and interactions (15,16) and is sensitive to sequestration of regulatory proteins (17).

Alternative splicing patterns can change significantly between tissues, developmental stages (18) during tumorigenesis (19) or other cellular transformation (20). In a single cell type, alternative splicing patterns can change in response to a change of environment, such as cellular stress (21,22), ischemia (23), nutritional status (24), neuronal activity (25–27) or receptor stimulation (28–30) (reviewed in 31). Sequence elements shared by different alternative exons indicate that environmental induced changes might be coordinated (32).

The stimulation of receptor tyrosine kinases can result in a change in splice site selection (28,33–36). With the exception of the CD44 model, where the signal was shown to be mediated by the ras-pathway (29), the connection between tyrosine phosphorylation and the spliceosome remains elusive. An increasing number of nuclear proteins were shown to be tyrosine phosphorylated and several tyrosine kinases and phosphatases are present in the nucleus (37), but the function of the phosphorylation is mostly unknown. Here we show that the nuclear protein YT521-B shuttles between the nucleus and the cytosol, where it is phosphorylated by SRC and TEC tyrosine kinase family members. Furthermore, YT521-B colocalizes with c-Abl in the nucleus and is tyrosine phosphorylated by c-Abl. Phosphorylation results in a translocation of the phosphorylated protein from nuclear YT bodies to the nucleoplasm and its association with an unsoluble nuclear fraction. YT521-B loses its ability to change splice site selection of the IL-4 receptor, CD44 and SRp20 pre-mRNA after phosphorylation, which is most likely due to its sequestration in an unsoluble, inactive state.

RESULTS

YT521-B is phosphorylated on tyrosine residues

YT521-B is a nuclear protein composed of several domains: four nuclear localization signals, a glutamic acid rich region of unknown function, the YTH domain that possibly binds nucleic acids, a proline rich domain containing putative SH3 domain binding sites and a glutamic acid/arginine-rich region involved in protein–protein interaction (7,8) (Fig. 1A). We have previously shown that protein–protein interactions between YT521-B and Sam68 are regulated by tyrosine phosphorylation and demonstrated that $p59^{fyn}$ causes phosphorylation of both proteins (7). Since YT521-B is detected only in the nucleus (8), we asked whether other non-receptor tyrosine kinases whose expression is often not only confined to the cell membrane can cause its phosphorylation (38). The sequencing of the human genome has demonstrated that humans possess 90 unique tyrosine kinases. Thirty-two of them are non-receptor type kinases which can be subdivided into 10 subfamilies (39). In unstimulated cells, the activity of the endogenous kinases can only be detected using phosphorylation-specific antibodies against specific target sites. To test the result of kinase activation, we increased their activity by transfecting cDNAs expressing the kinases. Previous studies of YT521-B were performed in HEK293

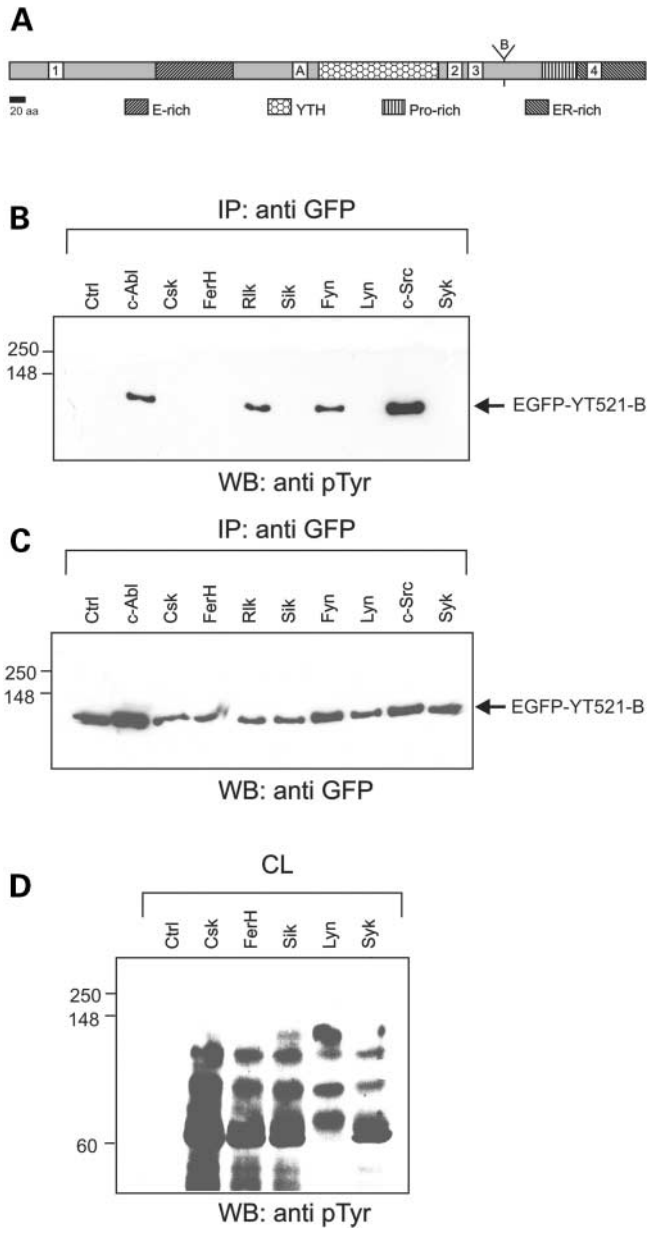

Figure 1. Several non-receptor tyrosine kinases phosphorylate YT521-B. (**A**) Domain structure of YT521-B. The four nuclear localization signals are indicated with numbers. The E-rich region, the ER-rich region, the proline rich region containing putative SH3 domains and YTH domain are indicated by different shading. The inserted A and B indicate the location of the alternative exons of YT521-B. (**B**) EGFP-YT521-B was cotransfected in HEK293 cells with expression clones of the kinases indicated. Protein was immunoprecipitated with anti GFP and tyrosine phosphorylation was detected with the antiphosphotyrosine antibody PY20. The reblot in (**C**) was performed with anti GFP to demonstrate the successful immunoprecipitation. The position of EGFP-YT521-B is indicated on the right. The molecular mass is given in kilodaltons on the left. (**D**) Crude lysates (CL) of cells transfected with kinases that do not phosphorylate YT521-B. The protein lysates were analyzed for tyrosine phosphorylation with PY20 to demonstrate the activity of the kinases employed.

cells (6,7,40) and we used these cells to allow for comparison of the data. A member of each subfamily was cotransfected with EGFP-YT521-B. After immunoprecipitation, tyrosine phosphorylation of YT521-B was detected by western blot using the phosphotyrosine specific antibody PY20. As shown in Figure 1B, the kinases c-Abl, Rlk, p59^{fyn} and c-Src, as members of the ABL, TEC and SRC families, phosphorylate YT521-B, whereas the related kinases Csk, FerH, Sik, Lyn and Syk, representing the CSK, FES, FRK and SYK families, had no effect. Similarly, Ack1, Ptk2 and Jtk1, representing the ACK, FAK and JTK families, did not phosphorylate YT521-B (data not shown). Reblotting (Fig. 1C) of the immunoprecipitates demonstrated the presence of YT521-B in all experiments, suggesting a specific action of c-Abl, Rlk, p59^{fyn} and c-Src. The kinases that did not phosphorylate YT521-B were active, as demonstrated by their ability to phosphorylate unknown proteins in cellular lysates (Fig. 1D). Together, our data show that YT521-B is phosphorylated by specific non-receptor tyrosine kinases.

YT521-B binds to c-Src and c-Abl kinases

Both c-Abl and Rlk phosphorylate YT521-B and can be located in the nucleus (41,42). Whereas c-Abl is expressed ubiquitously (43), Rlk expression is confined predominantly to T-lymphocytes (42). In contrast, c-Src and p59^{fyn} are ubiquitously expressed and located at the plasma membrane, although nuclear p59^{fyn} localization was observed during zebrafish development (44). We therefore investigated whether there is a direct molecular interaction between YT521-B and nuclear or membrane bound tyrosine kinases and tested whether YT521-B would coimmunoprecipitate with c-Abl or c-Src as ubiquitously expressed examples. First, we expressed FLAG-YT521-B in the presence of c-Abl and immunoprecipitated YT521-B using its FLAG-tag (Fig. 2A, left). As expected, in the presence of c-Abl, two bands are tyrosine phosphorylated (Fig. 2A, middle). The comparison with the western blot probed against YT521-B demonstrates that the lower band corresponds to FLAG-YT521-B (Fig. 2A, left). The reblot using an antibody against c-Abl shows that the upper band represents phosphorylated c-Abl (Fig. 2A, right). Next, we performed a similar experiment with c-Src (Fig. 2B) using EGFP-YT521-B. In the presence of c-Src, we observed the tyrosine phosphorylation of YT521-B (Fig. 2B, middle). Similar to c-Abl, we also detected phosphorylated c-Src in the YT521-B immunoprecipitate (Fig. 2B, middle), as confirmed by the reblot with anti Src antibody (Fig. 2B, right). Furthermore, we observed that recombinant c-Abl and c-Src can induce tyrosine phosphorylation of YT521-B generated in reticulate lysates (data not shown). We conclude that YT521-B can bind to c-Abl and c-Src in immunoprecipitation under *in vivo* conditions.

YT521-B shuttles between nucleus and cytoplasma

YT521-B was phosphorylated by the membrane bound kinases c-Src (Fig. 1) and p59^{fyn} (7), to which it binds in immunoprecipitation (Fig. 2) (7). Since YT521-B is detected only in the nucleus of cells, a phosphorylation by membrane bound kinases would only be possible during mitosis when the

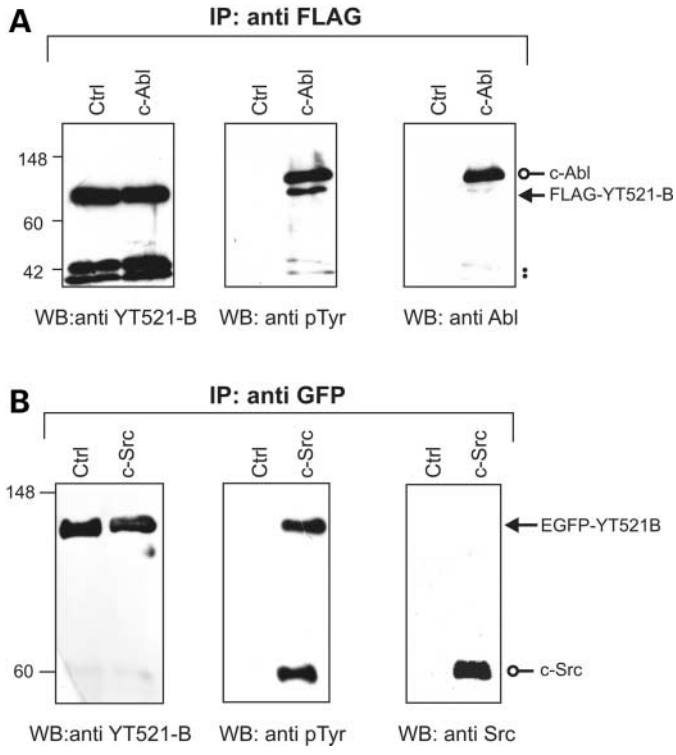

Figure 2. YT521-B binds to non-receptor tyrosine kinases. (**A**) YT521-B binds to c-Abl. Flag-YT521-B was coexpressed with or without a c-Abl expression construct in HEK293 cells. Proteins were immunoprecipitated with an anti-flag antibody. Immunoprecipitates were analyzed with antisera against YT521-B (PK2) (left), phosphotyrosine (PY20) (middle) and c-Abl (right). A pointed arrow indicates the localization of FLAG-YT521-B, an open round arrowhead shows the localization of c-Abl. Dots indicate the immunoglobulin bands. (**B**) YT521-B binds to c-Src. EGFP-YT521-B was coexpressed with or without a c-Src expression construct in HEK293 cells. Protein was immunoprecipitated with an anti GFP antibody. Immunoprecipitates were analyzed with antisera against YT521-B (PK2) (left), anti phosphotyrosine (PY20) (middle) and c-Src (right). A pointed arrow indicates the localization of EGFP-YT521-B, and an open round arrowhead shows the localization of c-Src.

nuclear structure disintegrates or would require shuttling of YT521-B between nucleus and cytosol that has been reported for several proteins implicated in splice site selection (45). To test these possibilities, we assessed the capability of EGFP-YT521-B to shuttle using a previously described cell fusion assay. The assay monitors accumulation of a fluorescent protein in acceptor nuclei of a newly formed polykaryon (46,47). Transfected HeLa cells expressing EGFP-YT521-B were fused with an excess of untransfected HeLa cells and accumulation of EGFP-YT521-B in acceptor nuclei monitored by time-lapse imaging. The donor cells were marked with red-fluorescent protein to allow distinction from acceptor cells. As shown in Figure 3, EGFP-YT521-B fluorescence is visible in the acceptor nuclei 28 min after cell fusion and increases by 308 min. Concomitantly, fluorescence intensity of the donor nucleus decreases (see Supplementary Material, movie). No shuttling is observed for GFP-tagged B23 (46) or histone 2B (data not shown) within 360 and 720 min, respectively, in this assay. These results indicate that YT521-B shuttles

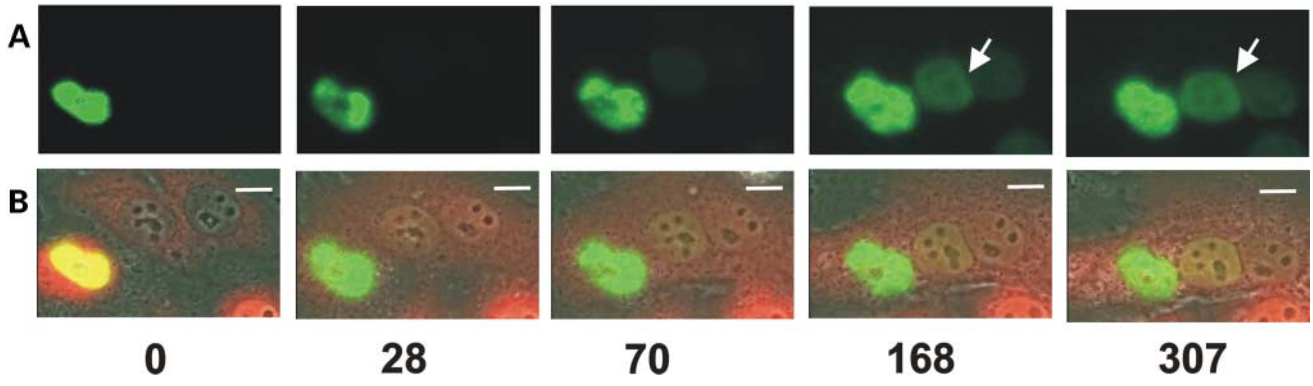

Figure 3. YT521-B shuttles between nucleus and cytosol. HeLa cells transfected with EGFP-YT521-B were fused to an excess of untransfected cells. (**A**) EGFP fluorescence at the time points in minutes after fusion indicated at the bottom. (**B**) The phase contrast images. An arrow indicates acceptor nuclei showing accumulation of EGFP-YT521-B. Numbers indicate the time after fusion in minutes. The scale bar is 10 μm. A movie showing this experiment and the decrease of EGFP-YT521-B in the donor nucleus is available in the Supplementary Material.

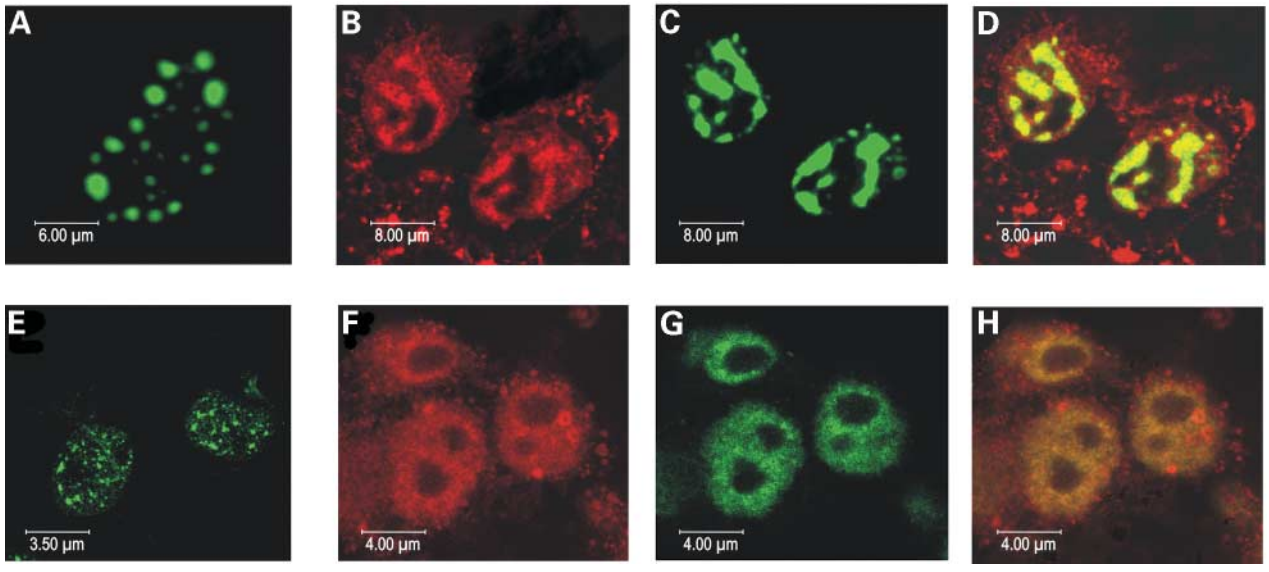

Figure 4. YT521-B colocalizes with c-Abl in the nucleus. (A–D) Overexpressed YT521-B colocalizes with c-Abl. EGFP-YT521-B is shown in green and c-Abl is stained in red. COS-7 cells were transiently transfected with EGFP-YT521-B. EGFP-YT521-B forms characteristic YT bodies (**A**). Cotransfected c-Abl localizes to the nucleus and can also be detected in the cytosol (**B**). In the presence of transfected c-Abl, YT521-B signal is spread throughout the nucleoplasm (**C**), excluding the nucleoli. Superimposition of the images in (B) and (C) shows nuclear colocalization between EGFP-YT521-B and c-Abl (**D**). (E–H) Endogenous YT521-B colocalizes with c-Abl. COS-7 cells were transfected with c-Abl and endogenous YT521-B (**E**) and c-Abl (**F**) was detected by immunocytochemistry. In the absence of transfected c-Abl, YT521-B forms characteristic YT bodies that are smaller than YT bodies formed after overexpression (E). Transfection of c-Abl causes dissolving of YT bodies (**G**). (**H**) Superimposition of the images in (F) and (G) that shows overlapping fluorescence in the nucleus. Cells were analyzed by confocal microscopy.

between nucleus and cytosol, where it could interact with membrane bound src-family kinases.

YT521-B colocalizes with c-Abl in the nucleus

Since c-Abl can coimmuoprecipitate with YT521-B, we next determined whether it colocalizes with YT521-B in the cell. YT521-B is present in a distinct nuclear substructure, the YT bodies (40). First, we determined the effect of c-Abl expression on overexpressed EGFP-YT521-B. In the absence of overexpressed c-Abl, EGFP-YT521-B is present in 20–30 nuclear dots, the YT bodies (Fig. 4A). After cotransfection with c-Abl, these dots dissolve and colocalize with c-Abl in the nucleus (Fig. 4C and D). As expected, c-Abl is also present in the cytosol (Fig. 4B). However, YT521-B is completely absent in the cytosol, demonstrating that overexpression of c-Abl does not induce a translocation of YT521-B into the cytosol (Fig. 4D). As reported earlier, EGFP-YT521-B generates YT bodies that appear larger then endogenous YT bodies (40). We therefore determined the influence of c-Abl on endogenous YT521-B localization (Fig. 4E), employing an antiserum that was previously

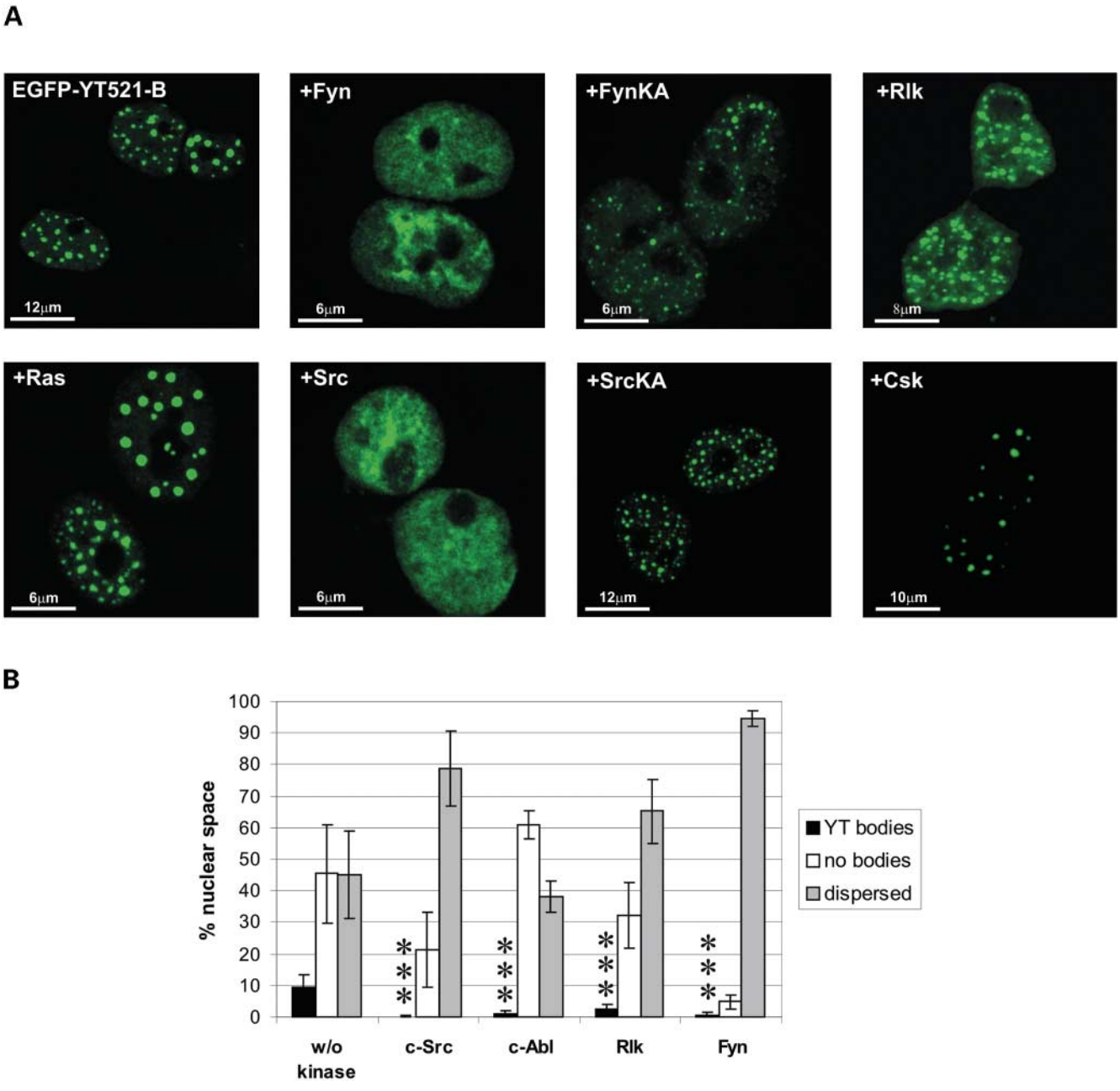

Figure 5. Phosphorylation of YT521-B dissolves YT bodies. EGFP-YT521-B was cotransfected with the kinases indicated. After 18 h, the formation of YT bodies was analyzed by confocal microscopy. (**A**) YT bodies formed by overexpressed EGFP-YT521-B dissolve after phosphorylation. EGFP-YT521-B was overexpressed in HEK293 cells in the presence of the kinases indicated. FynKA and SrcKA are K → A mutation in the kinase domains, resulting in inactive proteins. (**B**) Statistical evaluation of YT body formation in the presence of kinases. The nuclear areas containing YT bodies, diffuse nuclear staining and which were void of YT521-B signal were determined from 100 cells. Error bars indicate the standard deviations. The differences for YT body formation were statistically significant. The Student's *t*-test gave values of $P < 0.0001$ for all kinases, one-tailed *t*-values were 11.1, 10.0, 10.3 and 10.4 for c-Src, c-Abl, Rlk and $p59^{fyn}$, respectively.

developed (7,40). As shown in Figure 4H, endogenous YT521-B colocalizes with c-Abl in the nucleus, but not in the cytoplasm, where YT521-B is absent. In the presence of c-Abl (Fig. 4F), the defined YT bodies disperse throughout the nucleoplasm, excluding the nucleoli (Fig. 4G and H). Together with the coimmunoprecipitation, these data suggest that YT521-B is a target of c-Abl in the nucleus.

YT bodies disperse after tyrosine phosporylation

The effect of c-Abl on YT521-B is reminiscent of SR-protein kinases that cause dispersion of nuclear speckles containing their target SR-proteins (48). We therefore asked whether other tyrosine kinases phosphorylating YT521-B have a similar effect. We cotransfected EGFP-YT521-B with

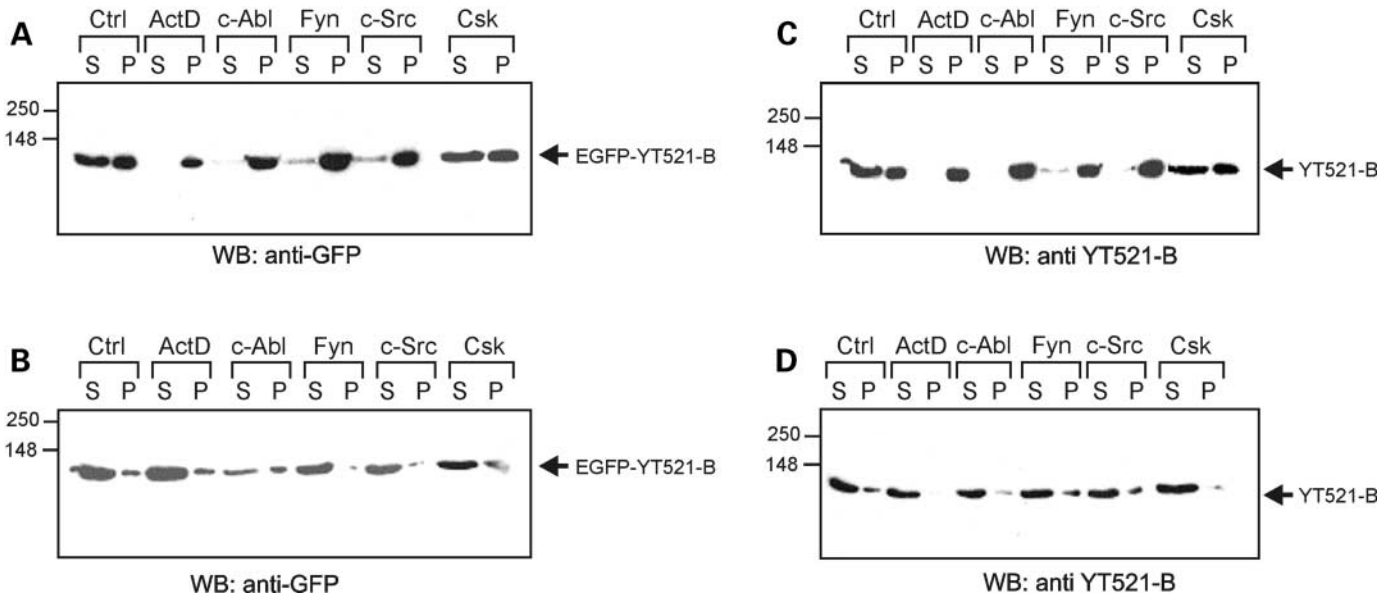

Figure 6. Phosphorylation of YT521-B influences its accumulation in a Triton X-100 insoluble nuclear compartment. The solubility of overexpressed EGFP-YT521 B was determined in the presence of actinomycin D, c-Abl, Fyn, c-Src and Csk in HNTG (**A**) and RIPA (**B**) buffer. The solubility of endogenous YT521-B was assayed in a similar way in HNTG (**C**) and RIPA (**D**) buffer. EGFP-YT521-B was coexpressed with c-Abl, p59^{fyn}, c-Src and Csk expression clones or EGFP-YT521-B expressing cells were treated with 50 μg/ml actinomycin D for 3 h. Cells were lysed in HNTG buffer (A) or RIPA buffer and benzonase (B). Equal amounts of the soluble fraction (S) or redissolved pellet fraction (P) were analyzed in 10% SDS–PAGE gels. Proteins were analyzed by western blot and ECL using the anti GFP antibody. Similar experiments were performed with endogenous YT521-B. Cells were transfected with c-Abl, p59^{fyn}, c-Src and Csk or treated with 50 μg/ml actinomycin D for 3 h and lysed in either HNTG buffer (C) or RIPA buffer and benzonase (D). The anti YT521-B antiserum was used to analyze western blots generated by loading equal amounts of the soluble fraction (S) or redissolved pellet fraction (P).

p59^{fyn}, c-Src and Rlk. These kinases phosphorylate YT521-B (Fig. 1). As shown in Figure 5A, coexpression of YT521-B with these kinases caused dispersion of YT bodies. As in the situation with c-Abl, YT521-B did not leave the nucleus or enter space occupied by nucleoli. Catalytic inactive mutants of p59^{fyn} or c-Src (FynKA, SrcKA) had no effect, which demonstrates that phosphorylation causes YT body dispersion. Activation of the ras-pathway that ultimately leads to phosporylation of SAM68 had no effect (29). Similarly, Csk that did phosphorylate some proteins, but not YT521-B (Fig. 1B and D) did not alter YT body formation (Fig. 5A). These results indicate that dispersion of YT bodies is dependent on YT521-B phosphorylation. However, we observed differences in nuclear staining after phosphorylation, as small dot-like structures were still visible after phosphorylation with Rlk. We therefore quantified the staining pattern and determined the nuclear space containing YT521-B bodies, diffuse YT521-B-staining and no YT521-B signal. YT bodies were defined as an accumulation of green signal stronger than the double standard deviation of the total signal distribution, which corresponds well with the visual inspection. As shown in Figure 5B, about 10% of the nuclear space is occupied by YT bodies in untreated cells. The presence of kinases reduced this number to 0–2.7%. The Student's *t*-test showed that these differences are statistically significant ($P < 0.0001$). The dispersion of YT bodies is concomitant with a change of the cellular areas where YT521-B is not present. It increases from 35–50% in untreated cells to 65–90% in Rlk, c-Src and p59^{fyn} transfected cells. In contrast, in c-Abl transfected cells, the area free of YT521-B slightly increases to 60%. It is possible that this is an effect of c-Abl overexpression that directs YT521-B to nuclear areas containing AT-rich DNA preferred by c-Abl for binding (43). These experiments show that the localization of YT521-B in YT bodies is regulated by tyrosine phosphorylation, similar to the localization of SR-proteins in nuclear speckles that is influenced by serine/threonine phosphorylation.

The solubility of YT521-B is regulated by phosphorylation

In the nucleus, YT521-B is present in two biochemically distinguishable compartments (40). The first compartment is YT bodies, which are soluble under non-denaturing conditions in Triton X-100 containing buffers. The remaining YT521-B protein resides diffusely in the nucleoplasm and is insoluble in Triton X-100 containing buffers. We previously demonstrated that YT521-B can translocate during the cell cycle or after actinomycin D treatment between these two compartments (40). High concentrations of actinomycin D (50 μg/ml) that block all three RNA polymerases cause complete dispersion of YT bodies and the accumulation of YT521-B in the Triton X-100 insoluble nuclear fraction (40). We therefore tested whether tyrosine phosphorylation of EGFP-YT521-B would also result in the accumulation of the protein in an insoluble nuclear fraction. We transfected EGFP-YT521-B into HEK293 cells and analyzed its solubility in a 1% Triton X-100-based cell lysis buffer (HNTG). As shown in Figure 6, in the presence of c-Abl, c-Src or p59^{fyn}, EGFP-YT521-B was present in the Triton insoluble pellet (P) fraction (Fig. 6A). In contrast, when

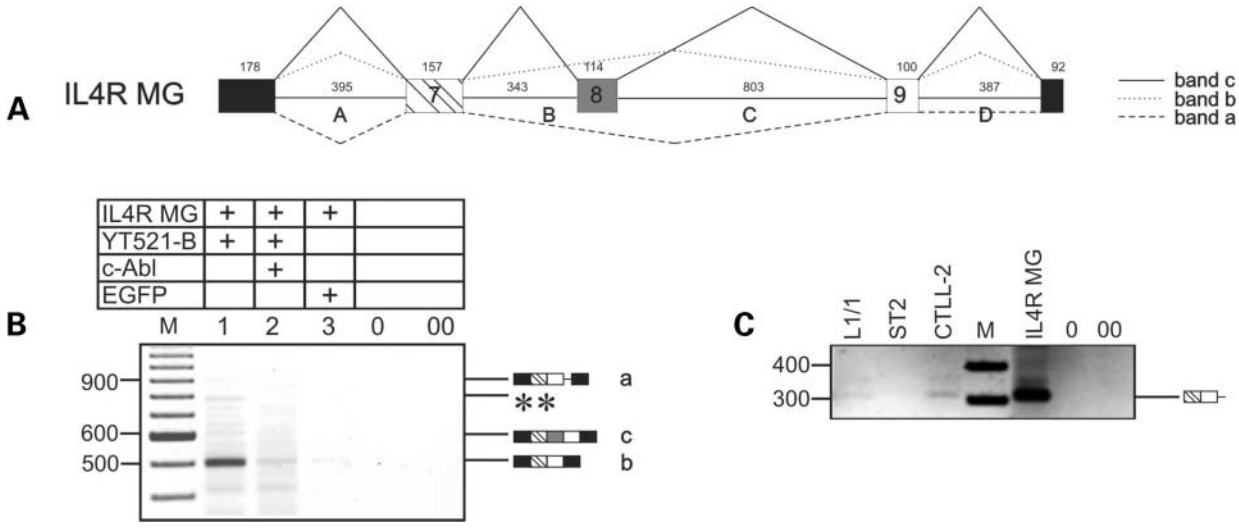

Figure 7. YT521-B is associated with the interleukin 4 receptor pre-mRNA. (**A**) Structure of the IL-4R minigene used. Exons are shown as boxes, introns as lines. The flanking insulin exons are shown in black, constitutive IL-4 receptor exons are shown in white or white-hatched boxes, the alternative interleukin 4 exon is indicated in gray. Numbers indicate the length of the introns and exons, letters indicate introns of the minigene construct. The splicing patterns are shown by different line styles. Bands a, b and c correspond to the bands in (B). (**B**) YT521-B immunoprecipitates contain interleukin 4 receptor pre-mRNA intermediates. The IL-4R minigene was cotransfected with EGFP-YT521-B. Protein–RNA complexes were isolated by immunoprecipitation with anti GFP in the absence of RNases. In lane 2, the c-Abl was cotransfected. Interleukin 4 receptor mRNA was detected by RT–PCR using minigene specific primers. 0: empty PCR control (water instead of RNA) 00: immunprecipitate without reverse transcriptase. (**C**) Retention of intron D exists *in vivo*. mRNAs from the lymphocyte cell lines L1/1, ST2 and CTLL-2 were analyzed by RT–PCR using primers in intron D and exon 7, which amplify the intron retention event (corresponding to band a) observed in the RNA-IPs.

we used a RIPA/benzonase buffer, the protein was present in the soluble (S) fraction (Fig. 6B), demonstrating that the protein is not covalently bound. This effect is dependent on YT521-B phosphorylation, as the presence of Csk that does not phosphorylate YT521-B, but does phosphorylate other proteins had no effect (Fig. 1B and D). Next, we determined whether endogenous YT521-B showed a similar response to tyrosine phosphorylation and analyzed its solubility in the presence of c-Abl, $p59^{fyn}$ and c-Src. As shown in Figure 6C, phosphorylation by these kinases resulted in YT521-B accumulation in a Triton X-100 insoluble compartment. Again, the phosphorylated protein was soluble in RIPA/benzonase containing buffer (Fig. 6D). We conclude that the tyrosine phosphorylation of YT521-B causes its association with insoluble nuclear structures.

YT521-B acts on the interleukin-4 receptor pre-mRNA

YT521-B has been shown to influence alternative splice site selection *in vivo* (7). Therefore, we wanted to investigate whether tyrosine phosphorylation would alter the ability of YT521-B to change splice site selection. Alternative splicing of the interleukin 4-receptor is regulated at least in part by tyrosine phosphorylation events emanating from stimulation of the IL-4 receptor by IL-4 (49). Due to alternative splicing and incorporation of an in-frame stop codon, a soluble and a membrane bound form of the IL-4 receptor are formed. The soluble form has no effect in mediating the IL-4 signal to the cell. We constructed a IL-4 receptor minigene comprising the alternative exon 8 of the mouse IL-4 receptor flanked by the constitutive exons 7 and 9 (50) using standard methods (51). The minigene cassette was cloned between the insulin exons of an exon-trap vector (Fig. 7A). First, we investigated whether YT521-B interacts with the IL-4 receptor mRNA *in vivo*. This is likely, because YT521-B binds to SAM68, rSLM-2, hnRNP G and SAF-B *in vivo*. All these proteins have been implicated in splice site selection (7). Furthermore, YT521-B can possibly bind nucleic acids via its YTH domain (8). We immunoprecpitated EGFP-YT521-B in the presence of the IL-4R minigene and detected RNA present in the precipitates by RT–PCR (52) using IL-4 receptor minigene specific primers. The amplification of IL-4 receptor variants demonstrates that YT521-B associates with this mRNA and can possibly regulate it (Fig. 7B). The presence of c-Abl reduced the amount of RNA found in the immunoprecipitates (Fig. 7B, lanes 1 and 2), although similar amounts of EGFP-YT521-B were present in the precipitates (data not shown). Sequencing of the products revealed that they were intermediates of the IL-4 receptor pre-mRNA processing (Fig. 7B). Interestingly, one of the products, band a, was generated by retention of intron D (Fig. 7A). To determine whether such an intron retention event occurs *in vivo*, we amplified RNA from various lymphocytes expressing the ILR receptor using an intron-specific primer. As shown in Figure 7C, mRNA with intron D retention is expressed in L1/1 and CTLL-2 cells (53). These data show that YT521-B interacts with the IL-4R pre-mRNA.

Phosphorylation changes the ability of YT521-B to influence splice site selection of the interleukin 4 pre-mRNA

Next, we determined whether YT521-B influences splice site selection of the IL-4R pre-mRNA. We analyzed IL-4R alternative splicing pattern dependency on YT521-B concentration by cotransfection and RT-PCR (51), using primers in

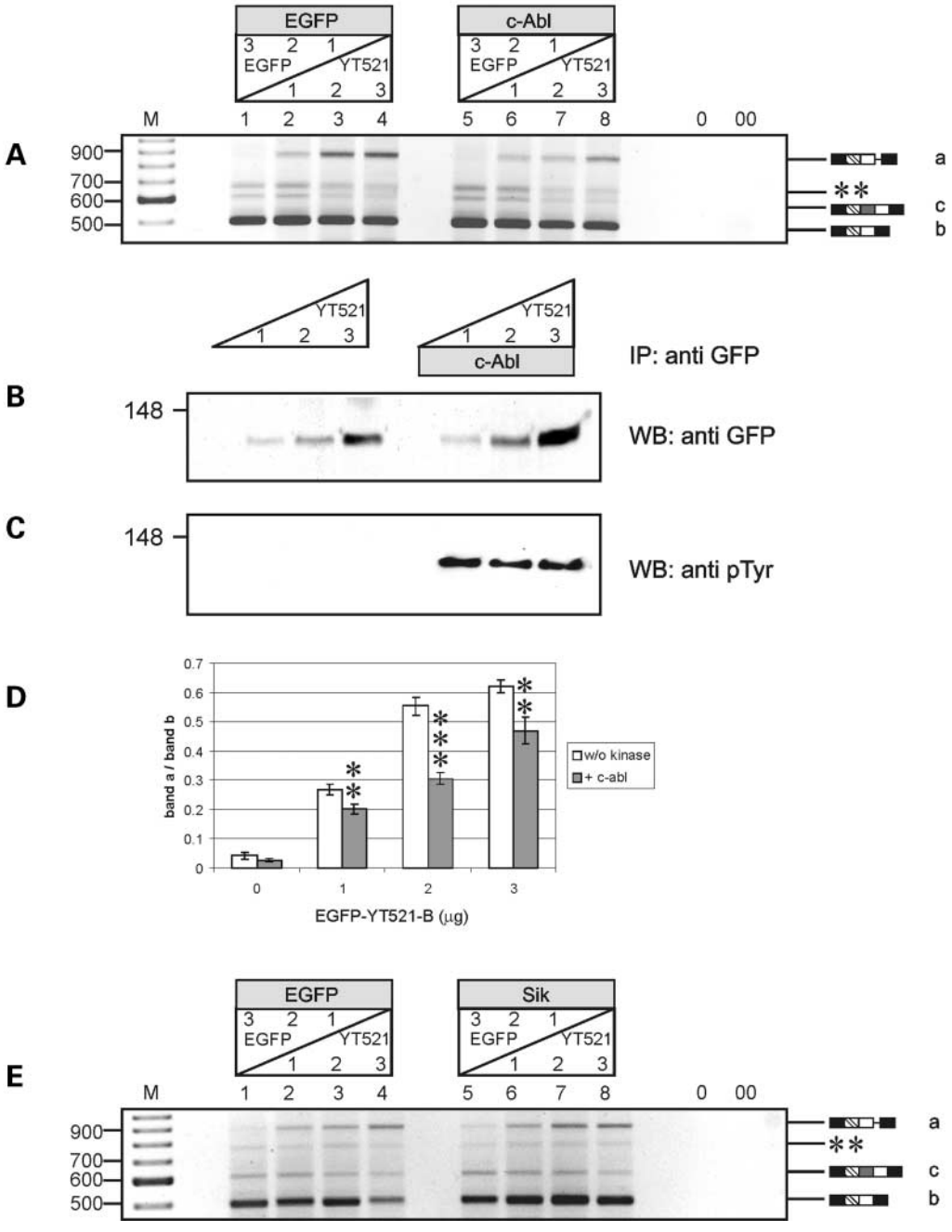

Figure 8. Phosphorylation of YT521-B changes its influence on interleukin 4 receptor splice site selection. (**A**) Influence of c-Abl on YT521-B mediated changes in splice site selection. HEK293 cells were transiently transfected with increasing amounts of EGFP-YT521-B in the presence of the IL-4R minigene (lanes 1–4). The amount of transfected EGFP-YT521-B is indicated and normalized using pEGFP-C2. An additional 0.5 μg EGFP-C2 was present in lanes 1–4 to allow comparison with the c-Abl cotransfections in lanes 5–8. In lanes 5–8, 0.5 μg of c-Abl expression plasmid was cotransfected with an increasing amount of EGFP-YT521-B. The RNA was analyzed by RT-PCR. 0, PCR without RT reaction; 00, PCR without template. The structure of the amplified products is indicated on the right; the alternative exon is shown in gray. M, 100 bp ladder. (**B**) The increase of YT521-B in the transfection assays was determined by immunoprecipitating EGFP-YT521-B with anti GFP. The protein was detected with anti-GFP. (**C**) Phosphorylation of YT521-B was detected with western blot, using an anti phosphotyrosine antibody on the immunoprecipitates of (B). (**D**) Statistical evaluation of the RT–PCR results. The ratio between the signal containing all constitutive exons as well as intron D to the signal of the band containing only constitutive exons [marked a and b in (A)] was determined from at least three different independent experiments. (**E**) Sik does not alter YT521-B mediated splice site selection. The experiment was performed as described in (A). Instead of c-Abl, an expression clone for Sik was employed.

the flanking constitutive insulin exons. Transfection of the IL-4R minigene in HEK239 resulted in a variant that predominantly skips the alternative exon 8 (Fig. 8A, lane 1). The cotransfection of c-Abl does not change the splicing pattern (Fig. 8A, lane 5) when no exogenous YT521-B is present. However, an increase in the concentration of YT521-B by cotransfection promotes retention of intron D in a dose dependent manner (Fig. 8A, lanes 2–4). The presence of c-Abl

significantly reduces this influence of YT521-B on alternative splice site selection (Fig. 8A, lanes 6–8). Western blots of immunoprecipitations made in parallel experiments confirmed the dose dependent increase of YT521-B (Fig. 8B) and verified that YT521-B was phosphorylated by c-Abl (Fig. 8C). Quantification of the RT–PCR experiments (Fig. 8D) revealed that the c-Abl evoked differences were statistically significant (*t*-test: $P < 0.0001$, $P < 0.006$) for 2 and 3 μg transfected EGFP-YT521-B, respectively (Fig. 8D). The observed 2- to 3-fold effect is comparable with the 1.5- to 4-fold effects of phosphorylation on splice site selection observed *in vivo* (21,31,54,55). To rule out that this is an unspecific tyrosine phosphorylation effect, we performed the same experiment in the presence of an expression clone for Sik, which does not phosphorylate YT521-B (Fig. 1B), but acts on non-identified cellular proteins (Fig. 1D). As shown in Figure 8E, Sik does not influence the YT521-B mediated changes in alternative splicing. We conclude that tyrosine phosphorylation of YT521-B changes its influence on IL-4R splice site selection. The phosphorylation dependency of the localization of YT521-B (Figs 5 and 6) suggests that changes in local concentration and solubility of YT521-B are responsible for these effects.

Phosphorylation changes the ability of YT521-B to influence CD44 and SRp20 alternative pre-mRNA splicing

To test whether the dependency of YT521-B function on its phosphorylation status is present in other systems, we tested two more minigenes. We employed the CD44 exon v5 minigene (Fig. 9A) that is dependent on the YT521-B interacting proteins rSLM-2 and SAM68 (28,29,56), as well as the SRp20 minigene pXB MG (Fig. 9D) that is regulated by YT521-B (7). As shown in Figure 9B, an increase of the concentration of YT521-B reduces inclusion of the alternative exon CD44 v5 in a concentration dependent manner. This dependency is partially abolished by c-abl induced phosphorylation, as c-abl does not influence the effect of small concentrations of YT521-B (Fig. 9B, lanes 2 and 6), but blocks the further increase of exon skipping promoted by YT521-B (Fig. 9B, lanes 3, 4 and 7, 8, and C). Similarly, phosphorylation modulates the effect of YT521-B on SRp20 alternative splicing. As shown in Figure 9E, lanes 1 and 5, in the presence of c-abl, exon 4 inclusion is increased, even when no additional YT521-B is transfected. It is possible that c-abl acts here on endogenous YT521-B. The presence of c-abl reduces the ability of YT521-B to decrease exon 4 usage 2-to 4-fold (Fig. 9E, lanes 2–4, 6–8, and F). Together, these data show that tyrosine phosphorylation modulates the influence of YT521-B on splice site selection of several pre-mRNAs.

DISCUSSION

Tyrosine-phosphorylation regulates the nuclear localization of YT521-B

An increasing number of specialized domains have been described for the nucleus. In several cases, these domains have been shown to be highly dynamic structures that respond to stimulation, changes in cell cycle, malignant transformation or DNA damage (reviewed in 1,4,57–59). The experiments described here show that the intranuclear distribution of YT521-B is dependent on its tyrosine phosphorylation status. Non-phosphorylated YT521-B is predominantly located in YT bodies, nuclear structures that contain focal sites of transcription and partially overlap with SC35 nuclear speckles (40). YT bodies are soluble in non-denaturing buffers. Tyrosine phosphorylation of YT521-B changes that distribution and solubility. It causes diffuse nuclear appearance of YT521-B and its tight association with an insoluble nuclear fraction. The release of YT521-B from YT bodies after tyrosine phosphorylation is reminiscent of the dispersion of nuclear speckles after serine/threonine phosphorylation of their proteins through cdc2 like kinases or SR-protein kinases (48,60–62). Functionally, serine/threonine phosphorylation of splicing factors can change splice site selection (17,63) by changing phosphorylation dependent protein–protein interactions (64). Since c-Abl causes YT521-B phosphorylation, colocalizes with it and binds tightly to it in immunoprecipitations, we propose that YT521-B is a novel nuclear target for c-Abl. It is possible that the first association between c-Abl and YT521-B is mediated by the proline rich region of YT521-B and the SH3 domain of c-Abl. Tyrosine phosphorylation would then stabilize the binding by phosphotyrosine–SH2 domain interaction. Several other non-receptor tyrosine kinases do not phosphorylate YT521-B, indicating a specific interaction between c-Abl and YT521-B. It is well established that RNA polII CTD is phosphorylated by c-Abl (65). Since YT bodies contain transcriptional start sites, it is possible that c-Abl phosphorylates YT521-B and RNA polII in the same nuclear compartment. The activity of nuclear c-Abl is controlled during the cell cycle via interaction with pRB (66). The cyclin dependent hyperphosphorylation of pRB releases binding to c-Abl and activates the kinase at the S-phase. This correlates with the finding that YT bodies cannot be detected during S-phase and form at the entrance of G1 (43,66). It also explains why YT bodies are markers for differentiated cells and are less pronounced in rapidly dividing transformed cells (40). In contrast to the CTD (65), YT521-B is phoshorylated by src family kinases. We observed shuttling of YT521-B between the nucleus and the cytosol, which shows that the protein can contact the membrane bound src-family kinases c-Src and $p59^{fyn}$ that phosphorylate YT521-B and bind to it tightly. It is therefore likely that these kinases can directly phosphorylate YT521-B and influence its properties. Computer programs predict 22 possible tyrosine phosphorylation sites in YT521-B. It remains to be determined which sites are responsible for the localization effects. The exact mechanism of actinomycin D influence on YT body localization remains to be determined as well. We did not observe a general increase in tyrosine phosphorylation after actinomycin D treatment, but cannot rule out the phosphorylation of specific proteins. Since YT521-B is insoluble after this treatment, it is not possible to determine whether it is phosphorylated. It is possible that actinomycin D causes a disruption of the nuclear matrix due to changes in DNA structure and RNA polymerase activity.

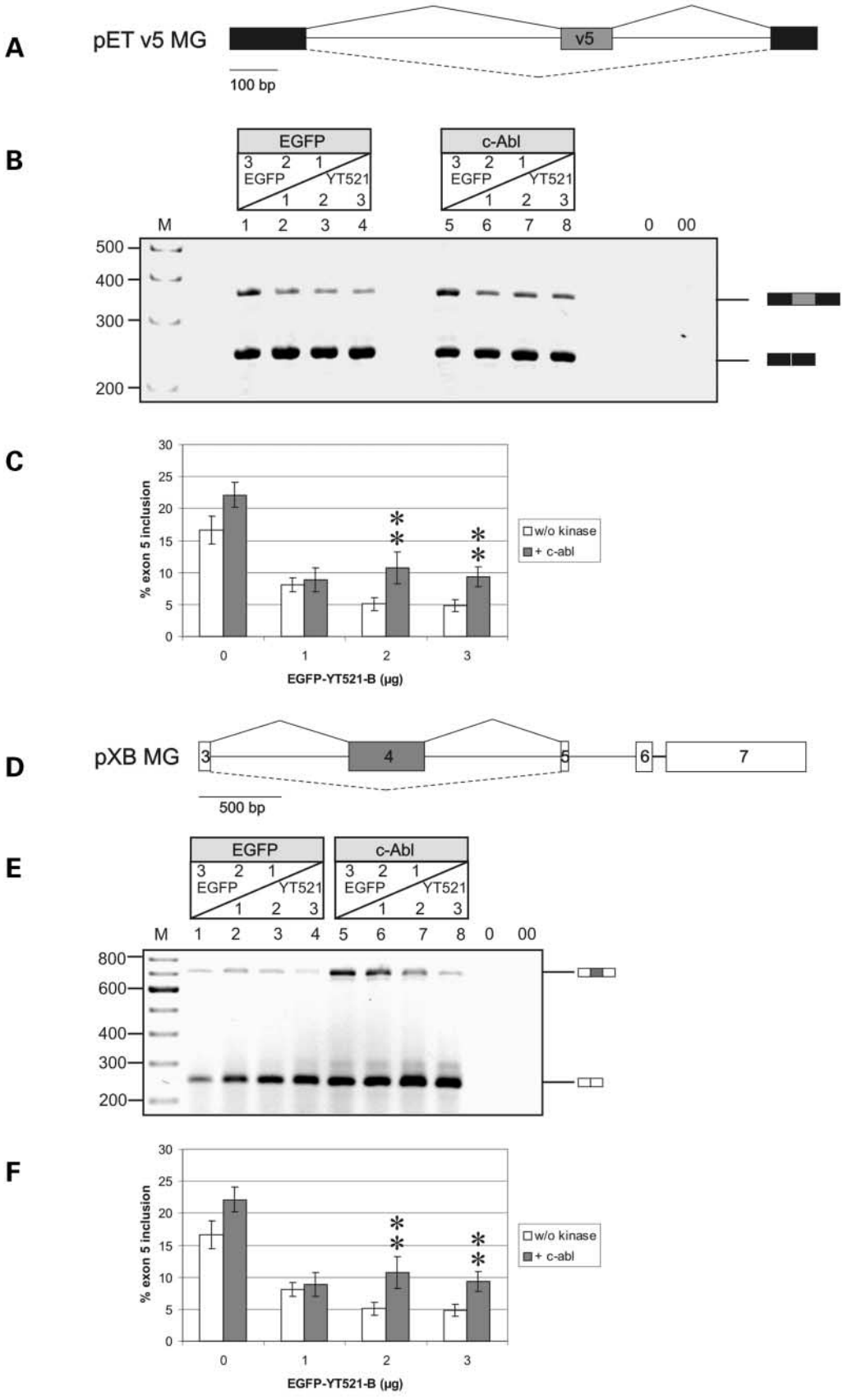

Similarities between effects of tyrosine phosphorylation in the cell membrane and the nucleus

After tyrosine phosphorylation, YT521-B changes its binding properties and associates with an insoluble nuclear structure. There are several parallels between the behavior of YT521-B and membrane bound receptor tyrosine kinases that form large signaling complexes after phosphorylation using scaffolding adaptors. First, in both cases tyrosine phosphorylation induces binding to other proteins. After phosphorylation, YT521-B binds tightly to c-Abl, most likely to the c-Abl SH2-domain. Secondly, the complex formation induced by phosphorylation changes the function of the molecules. Membrane bound receptor tyrosine kinases gain signaling function in the activated complexes, whereas YT521-B seems to lose its function in splice site regulation. It is not clear, however, whether there are nuclear scaffolding adaptor proteins in non-transformed cells. One possibility is that DNA or RNA present in the nuclear matrix serves as such an adaptor. All interacting proteins of YT521-B can bind to RNA, or to both RNA and matrix attachment region DNA (7). Biochemically, benzonase is needed to effectively solubilize phosphorylated YT521-B, which suggest an involvement of nucleic acids. Finally, there is no YT521-B ortholog in yeast or bacteria, suggesting that, similar to receptor tyrosine kinases (67), YT521-B is characteristic for metazoans.

Splice site selection is regulated by tyrosine phosphorylation

A functional consequence of YT521-B phosphorylation is to modulate the influence of YT521-B on splice site selection. YT521-B binds to several proteins implicated in splice site selection, which it can change in a concentration dependent manner (7). In the IL-4 receptor system that we used, YT521-B causes intron retention, which is a frequent form of alternative splicing occurring in an estimated 6% of all alternative splicing events (68). The retention of the intron between exon 9 and 10 can be detected in lymphocytes, indicating that it is a physiological event. However, the form is clearly low abundant in cells, especially when compared with the results from minigene transfection. This low abundance can be explained by in frame stop codons present in the intron that destine the mRNA to nonsense-mediated decay. RNA derived from minigenes most likely escapes nonsense-mediated decay because it is not translated, which explains the difference between minigene transfections and endogenous RNA. Phosphorylation changes the influence of YT521-B on splice site selection about 2- to 3-fold, which is comparable with the effects of phosphorylation on splice site selection observed *in vivo* (21,31,54,55). We observed a similar influence of phosphorylation on the ability of YT521-B to regulate the alternative cassette exons in CD44 and SRp20. This shows that this mechanism regulates not only intron retention, but also other modes of alternative splicing.

Non-phosphorylated YT521-B colocalizes with transcriptional start sites and shows overlapping localization with nuclear speckles (40). There, its most likely function is to bind nascent mRNA via its YTH domain (8) or to form specific mRNA–protein complexes that bridge splice sites (69,70). As with other splicing factors, interactions between YT521-B and other proteins functioning in pre-RNA processing is intrinsically weak (7). This allows for dynamic association and reassociation to the nascent pre-mRNA–protein complexes. Such a dynamic behavior is only possible when the protein is soluble. As a consequence, non-phosphorylated YT521-B can regulate splice sites in a concentration dependent manner. Phosphorylation results in such a strong association between YT521-B and nuclear structures that buffer conditions have to be used for solubilization which destroy all protein interactions of non-phosphorylated YT521-B. Furthermore, phosphorylated YT521-B is dispersed through the nucleus and removed from the vicinity of actively transcribed genes. Due to its insolublitity and spatial distance, phosphorylated YT521-B is effectively removed from pre-mRNA processing events in the cell and can no longer influence splice site selection. A similar phosphorylation-dependent redistribution of nuclear splicing factors has been demonstrated for SF2/ASF (45), where serine/threonine phosphorylation induced by the Clk/Sty kinases causes accumulation of SF2/ASF in the cytosol. Interestingly, the phosphorylation affects mainly the localization of proteins, but not their ability to change splice sites *in vitro* (71). Serine/threonine phosphorylation under stress conditions (22) or hypoxia (23) causes hyperphosphorylation and accumulation of SR-proteins or hnRNPs in the cytosol. This could serve the similar purpose of removing factors from pre-mRNA processing events. In fact, *in vivo*, splice site selection is altered after application of osmotic stress or hypoxia (22,23). Using cotransfection assays, we previously demonstrated that sequestration of splicing factors can regulate splice site selection (17). Although this mechanism

Figure 9. Phosphorylation of YT521-B changes splice site selection of CD44, exon v5 and SRp20, exon 4. (**A**) Structure of the CD44 v5 minigene used (76). Exons are shown as boxes, introns as lines. The flanking insulin exons are shown in black, the alternative CD44 exon v5 is indicated in gray. The splicing patterns are shown by different line styles. (**B**) Influence of c-Abl on YT521-B mediated changes in CD44 exon v5 splice site selection. HEK293 cells were transiently transfected with increasing amounts of EGFP-YT521-B in the presence of the CD44 v5 minigene (lanes 1–4). The amount of transfected EGFP-YT521-B is indicated and normalized using pEGFP-C2. An additional 0.5 μg EGFP-C2 was present in lanes 1–4 to allow comparison with the c-Abl cotransfections in lanes 5–8. In lanes 5–8, 0.5 μg of c-Abl expression plasmid was cotransfected with an increasing amount of EGFP-YT521-B. The RNA was analyzed by RT–PCR. 0, PCR without RT reaction; 00, PCR without template. The structure of the amplified products is indicated on the right; the alternative exon is shown in gray. M, 100 bp ladder. (**C**) Statistical evaluation of the RT–PCR results. The ratio between the signal corresponding to exon inclusion and all products was determined from at least three different independent experiments. Stars indicate statistical significant differences ($P = 0.005$ and $P = 0.001$, for 2 and 3 μg, respectively). (**D**) Structure of the SRp20 minigene used [pXB MG (77)]. Exons are shown as boxes, introns as lines. The alternative exon 4 is indicated in gray. The splicing patterns are shown by different line styles. (**E**) Influence of c-Abl on YT521-B mediated changes in SRp20 exon 4 splice site selection. HEK293 cells were transiently transfected with increasing amounts of EGFP-YT521-B in the presence of the pXB MG minigene (lanes 1–4). The other details are similar to (B). (**F**) Statistical evaluation of the RT–PCR results. The ratio between the signal corresponding to exon inclusion and all products was determined from at least three different independent experiments. Stars indicate statistical significant differences ($P = 0.0007$ and $P = 0.001$, for 2 and 3 μg, respectively).

can explain differences in splice site selection between tissues with different concentration of regulatory proteins, it cannot account for rapid changes in splice site selection after cellular stimulation (31). We propose that phosphorylation dependent sequestration of YT521-B in an insoluble state is a mechanism to regulate splice site selection in response to a kinase signal. After phosphorylation, YT521-B is localized in nuclear regions distant from the areas where transcription and pre-mRNA processing occurs. The phosphorylated protein is insoluble and most likely not able to participate in the dynamic rearrangement of protein complexes necessary for splice site recognition. This mechanism allows the cell to temporarily lower the active concentration of YT521-B without destroying the protein. The mechanism partially explains the frequently observed changes of splice site selection in malignant transformation (72) and during development (11), as these processes are triggered or are concomitant with an increase in receptor tyrosine phosphorylation. It implies that in addition to the combination of splicing factors (15) the tyrosine phosphorylation status of splicing factors can contribute to cell-specific alternative splicing.

MATERIALS AND METHODS

Cell culture and transfection

HEK293 and COS7 cells were maintained in DMEM supplemented with 10% fetal calf serum (GibcoBRL). For immunolabeling experiments, cells were grown on glass coverslips in 3.5 cm cell culture dishes. The day before transfection, 3.0×10^5 HEK293 cells per 3.5 cm plate were seeded in 3 ml of DMEM and 10% FCS and incubated at 37°C in 5% CO_2 for 24 h. Transient transfections of adherent HEK293 cells with cDNAs were performed using the calcium precipitation as described (51). COS7 cells were transfected 24 h after seeding using Superfect (Qiagen, Hilden, Germany) according to the manufacturer's instructions. Plasmids encoding for EGFP-YT521-B, FLAG-YT521-B contained the full length rat cDNA with N-terminal tags and were described earlier (7), as well as expression constructs for c-Abl (human), Csk, c-Fyn, c-FynKA, c-Src and c-SrcKA (7). FerH expressed from pHUG10–3 (Fer) was generously supplied by N. Heisterkamp (73), Rlk from pcDNA3-RLK from P.L. Schwartzberg (42), Sik was provided by A.L. Tyner (74), Syk from pSVL-Syk from J. Zhang (75).

Immunoprecipitation and western blotting

Twenty-four hours after transfection, cells were lysed in 200 µl of radioimmunoprecipitation assay (RIPA) buffer (1% NP40, 1% sodium deoxycholate, 0.1% SDS, 150 mM NaCl, 10 mM Na-phosphate, pH 7.2, 2 mM EDTA, 50 mM NaF, 5 mM β-glycerolphosphate, and freshly added 4 mM sodium orthovanadate, 1 mM DTT, 1 mM PMSF, 20 µg/ml aprotinin, and 100 U/ml benzonase) for 30 min on ice. Precipitates were cleared by centrifugation. Lysates were diluted 4-fold in RIPA rescue (20 mM NaCl, 10 mM Na-phosphate, pH 7.2, 1 mM NaF, 5 mM β-glycerolphosphate, and freshly added 2 mM sodium orthovanadate, 1 mM DTT, 1 mM PMSF, and 20 µg/ml aprotinin). Immunoprecipitations were performed overnight at 4°C with agitation using anti GFP (Roche) or anti FLAG (Sigma) antibodies and protein A-Sepharose (Pharmacia; protein A-Sepharose : Sepharose, 1 : 1, resuspended in RIPA rescue buffer), followed by three washes in 50 mM HEPES, pH 7.5, 150 mM NaCl, 1 mM EDTA, 10% glycerol, 0.1% Triton X-100, and freshly added 2 mM sodium orthovanadate, 100 mM NaF, 1 mM PMSF, and 20 µg/ml aprotinin. The proteins were subsequently analyzed on 7.5 or 10% SDS–polyacrylamide gels followed by western blotting and ECL. Anti GFP (Roche), antiphosphotyrosine 4G10 (Santa Cruz), anti-YT521-B (40), Anti Abl (21–11, Santa Cruz), FLAG M2 (Sigma) and anti Src antibodies (pp60src, Biomol, Germany) were used according to the manufacturer's instructions. Anti YT521-B (PK2) was described earlier (40).

Protein shuttling

Protein shuttling was essentially performed as described (46). Briefly, HeLa cells were transfected with plasmids directing expression of EGFP-YT521-B and red fluorescent protein (RFP) which served as fusion control. Transfected HeLa cells were cultured with an excess of untransfected HeLa cells and fusion induced by treatment with polyethylene glycol 1500 (Roche Diagnostics, Mannheim, Germany) for 180 s. Fluorescence was monitored by real-time imaging using the Zeiss 'Cell Observer', a temperature-controlled Zeiss Axiovert 200M research microscopy (Carl Zeiss, Goettingen) with scanning stage, CO_2-incubation and Software AxioVision 4.1 (Carl Zeiss Vision, Hallbergmoos). Images were acquired with a 40× Plan Neofluar Objective and the filter sets 'Zeiss No. 44' (475/40 FT 500 BP530/50) and 'Zeiss No. 43' (545/25 FT 570 BP605/70) used to visualize GFP- and RFP-fluorescence, respectively.

Solubility assay

The solubility assay was previously described (60). Twenty-four hours after transfection, cells were lysed for 30 min on ice in 200 µl buffer containing 50 mM Hepes, pH 7.5, 150 mM NaCl, 1% Triton X-100, 10% glycerol, 1 mM EDTA, 20 mM sodium pyrophosphate, 2 mM sodium orthovanadate, 100 mM NaF, 5 mM ß-glycerophosphate, 1 mM PMSF and 1 µg/ml aprotinin (HNTG buffer). The lysates were centrifuged at 13 000*g* for 15 min at 4°C, 100 µl 3× SDS sample buffer was added to the supernatant, and 300 µl 3× SDS sample buffer was added to the remaining pellet. The probes were mixed, boiled for 5 min, and 30 µl of each fraction loaded onto 10% SDS–polyacrylamide gels. Alternatively, cells were lysed for 30 min on ice in 200 µl RIPA buffer (0.01 M sodium phosphate, 1% NP-40, 1% sodium deoxycholate, 0.1% SDS, 0.15 M NaCl, 2 mM EDTA, 1 mM NaF, 4 mM sodium orthovanadate, 5 mM ß-glycerolphosphate, 1 mM PMSF, 1 µg/ml aprotinin, and 100 U/ml benzonase). Lysates were centrifuged for 15 min at 4°C, 100 µl 3× SDS sample buffer was added to the supernatant, and 300 µl 3× SDS sample buffer was added to the pellet. An aliquot of 30 µl of the fraction was loaded in each lane and analyzed on 10% SDS–polyacrylamide gels. The proteins were analyzed

by western blotting and ECL using anti-GFP (Roche) and PK2 antibodies.

Immunostaining

Cells were fixed in 4% formaldehyde and PBS for 10 min at 4°C, washed three times in PBS and 0.1% Triton X-100, and blocked in PBS, 0.1% Triton X-100, and 3% NGS for 2 h at room temperature. Cells were then incubated with the appropriate antibody (diluted in PBS, 0.1% Triton X-100, and 3% bovine serum albumin) overnight at 4°C and washed three times in PBS and 0.1% Triton X-100. Cells were then incubated with CY3- or FITC-coupled secondary antibody (Dianova) in PBS and 0.1% Triton X-100 for 2 h at room temperature, washed three times in PBS and 0.1% Triton X-100, and mounted on glass slides in Fluormount (Dianova). The cells were examined by laser scanning fluorescent microscopy (Leica).

Quantification of cell staining

Cells were analyzed with confocal microscopy and single images were analyzed using Photoshop. First the cell nucleus was outlined. Next, YT bodies were marked through visual inspection and the mean of their integrated signals − standard deviations was calculated as YT bodies. The black areas were marked by visual inspection and the mean of their integrated distribution + standard deviation was designated as areas void of YT521-B. The remaining area was defined as dispersed YT521-B staining.

RNA immunoprecipitation

Cells were trypsinated 36 h after transfection and washed in 30 vol of PBS and resuspended in one packed cell volume of buffer A (10 mM HEPES, pH 8.0, 1.5 mM $MgCl_2$, 10 mM KCl, 1 mM DTT) and allowed to swell on ice for 15 min. Cells were lysed with a 23G hypodermic needle and nuclei were recovered by 20 s centrifugation at 12 000*g* at RT. The crude nuclear pellet was resuspended in two-thirds of one packed cell volume of buffer C [20 mM HEPES, pH 8.0, 25% (v/v) glycerol, 420 mM NaCl, 0.2 mM EDTA, pH 8.0, 1 mM DTT, 0.5 mM PMSF] and incubated at 4°C with stirring for 30 min. The nuclear debris was pelleted by 5 min centrifugation at 12 000*g*. Collected nuclei were resuspended in 0.6 ml of NET-Triton (150 mM NaCl, 50 mM Tris-HCl, pH 7.4, 0.1% Triton X-100, protease inhibitors), pushed through a narrow-gauge needle and centrifuged. Immunoprecipitation with anti GFP antibody and protein A Sepharose was performed overnight at 4°C on the supernatant, followed by five washes with cold RIPA buffer. RNA was isolated using the Trizol (Invitrogen) reagent. After ethanol precipitation the RNA pellet was dissolved in RNase-free water.

In vivo splicing assay

In vivo splicing was performed as described (51). Briefly, 1 μg of the reporter gene was transfected together with an increasing amount (0, 1, 2 and 3 μg) of YT521-B-construct and 0.5 μg of c-Abl plasmid in 300 000 HEK293 cells using the calcium phosphate method. Empty vector (pEGFP-C2) was added to ensure that equal amounts of DNA were transfected. Transfection was performed at 37°C in 3% CO_2 overnight. RNA was isolated 17 h after transfection using an RNeasy mini kit (Qiagen), following the manufacturer's instructions. RNA was eluted in 40 μl of RNase-free H_2O. For reverse transcription, 2 μl of isolated RNA were mixed with 5 pmol of antisense minigene-specific primer in 0.5 μl H_2O, 2 μl of 5× RT buffer, 1 μl of 100 mM DTT, 1 μl of 10 mM dNTP, 3 μl of H_2O, 0.25 μl of RNase inhibitor and 0.2 μl of SuperScriptII (Invitrogen). The tubes were incubated for 45 min at 42°C. Aliquots of 1 μl of the RT reaction were mixed with 2.5 pmol of sense and antisense primer each, 10× PCR reaction buffer, 200 μM dNTP and 0.2 μl *Taq*-polymerase. For the IL4R minigene, the PCR conditions were initial denaturation for 2 min at 94°C; 35 cycles: 30 s denaturation at 94°C, combined annealing and extension at 72°C for 90 s, after 35 cycles a final extension at 72°C for 20 min and cooling to 4°C in a Perkin-Elmer thermocycler. The PCR reaction products were analyzed on a 2% agarose Tris borate-EDTA gel of thickness 0.3–0.4 cm.

SUPPLEMENTARY MATERIAL

Supplementary Material is available at HMG Online.

ACKNOWLEDGEMENTS

We thank Nora Heisterkamp, Pamela Schwartzberg, G. Superti-Furga, A.L. Tyner and J. Zhang for providing expression clones and Andre Gessner for providing c-DNAs. This work was supported by the Deutsche Forschungsgemeinschaft.

REFERENCES

1. Spector, D.L. (2001) Nuclear domains. *J. Cell Sci.*, **114**, 2891–2893.
2. Sacco-Bubulya, P. and Spector, D.L. (2002) Disassembly of interchromatin granule clusters alters the coordination of transcription and pre-mRNA splicing. *J. Cell Biol.*, **156**, 425–436.
3. Misteli, T., Cáceres, J.F. and Spector, D.L. (1997) The dynamics of a pre-mRNA splicing factor in living cells. *Nature*, **387**, 523–527.
4. Lamond, A.I. and Spector, D.L. (2003) Nuclear speckles: a model for nuclear organelles. *Nat. Rev. Mol. Cell Biol.*, **4**, 605–612.
5. Iborra, F.J. and Cook, P.R. (2002) The interdependence of nuclear structure and function. *Curr. Opin. Cell Biol.*, **14**, 780–785.
6. Imai, Y., Matsuo, N., Ogawa, S., Tohyama, M. and Takagi, T. (1998) Cloning of a gene, YT521, for a novel RNA splicing-related protein induced by hypoxia/reoxygenation. *Brain Res. Mol. Brain Res.*, **53**, 33–40.
7. Hartmann, A.M., Nayler, O., Schwaiger, F.W., Obermeier, A. and Stamm, S. (1999) The interaction and colocalization of Sam68 with the splicing- associated factor YT521-B in nuclear dots is regulated by the Src family kinase p59(fyn). *Mol. Biol. Cell*, **10**, 3909–3926.
8. Stoilov, P., Rafalska, I. and Stamm, S. (2002) YTH: a new domain in nuclear proteins. *Trends Biochem. Sci.*, **27**, 495–496.
9. Modrek, B., Resch, A., Grasso, C. and Lee, C. (2001) Genome-wide detection of alternative splicing in expressed sequences of human genes. *Nucl. Acids Res.*, **29**, 2850–2859.
10. Johnson, J.M., Castle, J., Garrett-Engele, P., Kan, Z., Loerch, P.M., Armour, C.D., Santos, R., Schadt, E.E., Stoughton, R. and Shoemaker,

D.D. (2003) Genome-wide survey of human alternative pre-mRNA splicing with exon junction microarrays. *Science*, **302**, 2141–2144.
11. Black, D.L. (2003) Mechanisms of Alternative Pre-Messenger RNA Splicing. *Annu. Rev. Biochem.*, **72**, 291–336
12. Cramer, P., Srebrow, A., Kadener, S., Werbajh, S., de la Mata, M., Melen, G., Nogues, G. and Kornblihtt, A.R. (2001) Coordination between transcription and pre-mRNA processing. *FEBS Lett.*, **498**, 179–182.
13. Cartegni, L., Chew, S.L. and Krainer, A.R. (2002) Listening to silence and understanding nonsense: exonic mutations that affect splicing. *Nat. Rev. Genet.*, **3**, 285–298.
14. Maniatis, T. and Tasic, B. (2002) Alternative pre-mRNA splicing and proteome expansion in metazoans. *Nature*, **418**, 236–243.
15. Smith, C.W. and Valcarcel, J. (2000) Alternative pre-mRNA splicing: the logic of combinatorial control. *Trends Biochem. Sci.*, **25**, 381–388.
16. Roberts, G.C. and Smith, C.W. (2002) Alternative splicing: combinatorial output from the genome. *Curr. Opin. Chem. Biol.*, **6**, 375–383.
17. Stoilov, P., Daoud, R., Nayler, O. and Stamm, S. (2004) Human tra2-beta1 autoregulates its protein concentration by influencing alternative splicing of its pre-mRNA. *Hum. Mol. Genet.*, **13**, 509–524.
18. Thanaraj, T.A., Stamm, S., Clark, F., Riethoven, J.J., Le Texier, V. and Muilu, J. (2004) ASD: the Alternative Splicing Database. *Nucl. Acids Res.*, **32**, D64–69.
19. Xu, Q., Modrek, B. and Lee, C. (2002) Genome-wide detection of tissue-specific alternative splicing in the human transcriptome. *Nucl. Acids Res.*, **30**, 3754–3766.
20. Stoilov, P., Meshorer, E., Gencheva, M., Glick, D., Soreq, H. and Stamm, S. (2002) Defects in pre-mRNA processing as causes of and predisposition to diseases. *DNA Cell Biol.*, **21**, 803–818.
21. Meshorer, E., Erb, C., Gazit, R., Pavlovsky, L., Kaufer, D., Friedman, A., Glick, D., Ben-Arie, N. and Soreq, H. (2002) Alternative splicing and neuritic mRNA translocation under long-term neuronal hypersensitivity. *Science*, **295**, 508–512.
22. van der Houven van Oordt, W., Diaz-Meco, M.T., Lozano, J., Krainer, A.R., Moscat, J. and Caceres, J.F. (2000) The MKK(3/6)-p38-signaling cascade alters the subcellular distribution of hnRNP A1 and modulates alternative splicing regulation. *J. Cell Biol.*, **149**, 307–316.
23. Daoud, R., Mies, G., Smialowska, A., Oláh, L., Hossmann, K. and Stamm, S. (2002) Ischemia induces a translocation of the splicing factor tra2-beta1 and changes alternative splicing patterns in the brain. *J. Neurosci.*, **22**, 5889–5899.
24. Amir-Ahmady, B. and Salati, L.M. (2001) Regulation of the processing of glucose-6-phosphate dehydrogenase mRNA by nutritional status. *J. Biol. Chem.*, **276**, 10 514–10 523.
25. Daoud, R., Da Penha Berzaghi, M., Siedler, F., Hubener, M. and Stamm, S. (1999) Activity-dependent regulation of alternative splicing patterns in the rat brain. *Eur. J. Neurosci.*, **11**, 788–802.
26. Xie, J. and Black, D.L. (2001) A CaMK IV responsive RNA element mediates depolarization-induced alternative splicing of ion channels. *Nature*, **410**, 936–939.
27. Stork, O., Stork, S., Pape, H.C. and Obata, K. (2001) Identification of genes expressed in the amygdala during the formation of fear memory. *Learn. Mem.*, **8**, 209–219.
28. Weg-Remers, S., Ponta, H., Herrlich, P. and Konig, H. (2001) Regulation of alternative pre-mRNA splicing by the ERK MAP-kinase pathway. *EMBO J.*, **20**, 4194–4203.
29. Matter, N., Herrlich, P. and Konig, H. (2002) Signal-dependent regulation of splicing via phosphorylation of Sam68. *Nature*, **420**, 691–695.
30. Chalfant, C.E., Watson, J.E., Bisnauth, L.D., Kang, J.B., Patel, N., Obeid, L.M., Eichler, D.C. and Cooper, D.R. (1998) Insulin regulates protein kinase CbetaII expression through enhanced exon inclusion in L6 skeletal muscle cells. A novel mechanism of insulin- and insulin-like growth factor-i-induced 5′ splice site selection. *J. Biol. Chem.*, **273**, 910–916.
31. Stamm, S. (2002) Signals and their transduction pathways regulating alternative splicing: a new dimension of the human genome. *Hum. Mol. Genet.*, **11**, 2409–2416.
32. Rothrock, C., Cannon, B., Hahm, B. and Lynch, K.W. (2003) A conserved signal-responsive sequence mediates activation-induced alternative splicing of CD45. *Mol. Cell*, **12**, 1317–1324.
33. Shifrin, V.I. and Neel, B.G. (1993) Growth factor-inducible alternative splicing of nontransmembrane phosphotyrosine phosphatase PTP-1B pre-mRNA. *J. Biol. Chem.*, **268**, 25376–25384.
34. Ishizuka, T., Kajita, K., Yamada, K., Miura, A., Kanoh, Y., Ishizawa, M., Wada, H., Itaya, S., Yamamoto, M., Yasuda, K. *et al.* (1996) Insulin regulated PKC isoform mRNA in rat adipocytes. *Diabetes Res. Clin. Pract.*, **33**, 159–167.
35. Scotet, E. and Houssaint, E. (1998) Exon III splicing switch of fibroblast growth factor (FGF) receptor-2 and -3 can be induced by FGF-1 or FGF-2. *Oncogene*, **17**, 67–76.
36. Smith, M.A., Fanger, G.R., O'Connor, L.T., Bridle, P. and Maue, R.A. (1997) Selective regulation of agrin mRNA induction and alternative splicing in PC12 Cells by Ras-dependent actions of nerve growth factor. *J. Biol. Chem.*, **272**, 15675–15681.
37. Cans, C., Mangano, R., Barila, D., Neubauer, G. and Superti-Furga, G. (2000) Nuclear tyrosine phosphorylation: the beginning of a map. *Biochem. Pharmacol.*, **60**, 1203–1215.
38. Pendergast, A.M. (1996) Nuclear tyrosine kinases: from Abl to Wee1. *Curr. Opin. Cell Biol.*, **8**, 174–181.
39. Robinson, D.R., Wu, Y.-M. and Lin, S.-F. (2000) The protein tyrosine kinase family of the human genome. *Oncogene*, **19**, 5548–5557.
40. Nayler, O., Hartmann, A.M. and Stamm, S. (2000) The ER-repeat protein YT521-B localizes to a novel subnuclear compartment. *J. Cell Biol.*, **150**, 949–961.
41. Taagepera, S., McDonald, D., Loeb, J.E., Whitaker, L.L., McElroy, A.K., Wang, J.Y. and Hope, T.J. (1998) Nuclear-cytoplasmic shuttling of C-ABL tyrosine kinase. *Proc. Natl Acad. Sci. USA*, **95**, 7457–7462.
42. Debnath, J., Chamorro, M., Czar, M.J., Schaeffer, E.M., Lenardo, M.J., Varmus, H.E. and Schwartzberg, P.L. (1999) rlk/TXK encodes two forms of a novel cysteine string tyrosine kinase activated by Src family kinases. *Mol. Cell. Biol.*, **19**, 1498–1507.
43. Van Etten, R.A. (1999) Cycling, stressed-out and nervous: cellular functions of c-Abl. *Trends Cell Biol.*, **9**, 179–186.
44. Rongish, B.J. and Kinsey, W.H. (2000) Transient nuclear localization of Fyn kinase during development in zebrafish. *Anat. Rec.*, **260**, 115–123.
45. Caceres, J.F., Screaton, G.R. and Krainer, A.R. (1998) A specific subset of SR proteins shuttles continously between the nucleus and the cytoplasm. *Genes Dev.*, **12**, 55–66.
46. Neumann, M., Afonina, E., Ceccherini-Silberstein, F., Schlicht, S., Erfle, V., Pavlakis, G.N. and Brack-Werner, R. (2001) Nucleocytoplasmic transport in human astrocytes: decreased nuclear uptake of the HIV Rev shuttle protein. *J. Cell Sci.*, **114**, 1717–1729.
47. Lee, S., Neumann, M., Stearman, R., Stauber, R., Pause, A., Pavlakis, G.N. and Klausner, R.D. (1999) Transcription-dependent nuclear-cytoplasmic trafficking is required for the function of the von Hippel-Lindau tumor suppressor protein. *Mol. Cell. Biol.*, **19**, 1486–1497.
48. Colwill, K., Pawson, T., Andrews, B., Prasad, J., Manley, J.L., Bell, J.C. and Duncan, P.I. (1996) The Clk/Sty protein kinase phosphorylates SR splicing factors and regulates their intranuclear distribution. *EMBO J.*, **15**, 265–275.
49. Blum, H., Wolf, M., Enssle, K., Rollinghoff, M. and Gessner, A. (1996) Two distinct stimulus-dependent pathways lead to production of soluble murine interleukin-4 receptor. *J. Immunol.*, **157**, 1846–1853.
50. Wrighton, N., Campbell, L.A., Harada, N., Miyajima, A. and Lee, F. (1992) The murine interleukin-4 receptor gene: genomic structure, expression and potential for alternative splicing. *Growth Factors*, **6**, 103–118.
51. Stoss, O., Stoilov, P., Hartmann, A.M., Nayler, O. and Stamm, S. (1999) The *in vivo* minigene approach to analyze tissue-specific splicing. *Brain Research Protocols*, **4**, 383–394.
52. Buckanovich, R.J. and Darnell, R.B. (1997) The neuronal RNA binding protein Nova-1 recognizes specific RNA targets *in vitro* and *in vivo*. *Mol. Cell. Biol.*, **17**, 3194–3201.
53. Schnare, M., Blum, H., Juttner, S., Rollinghoff, M. and Gessner, A. (1998) Specific antagonism of type I IL-4 receptor with a mutated form of murine IL-4. *J. Immunol.*, **161**, 3484–3492.
54. Abdennebi, L., Lesport, A.S., Remy, J.J., Grebert, D., Pisselet, C., Monniaux, D. and Salesse, R. (2002) Differences in splicing of mRNA encoding LH receptor in theca cells according to breeding season in ewes. *Reproduction*, **123**, 819–826.
55. Holdiman, A.J., Fergus, D.J. and England, S.K. (2002) 17beta-Estradiol upregulates distinct maxi-K channel transcripts in mouse uterus. *Mol. Cell. Endocrinol.*, **192**, 1–6.
56. Stoss, O., Olbrich, M., Hartmann, A.M., Konig, H., Memmott, J., Andreadis, A. and Stamm, S. (2001) The STAR/GSG family protein

rSLM-2 regulates the selection of alternative splice sites. *J. Biol. Chem.*, **276**, 8665–8673.
57. Matera, A.G. (1999) Nuclear bodies: multifaceted subdomains of the interchromatin space. *Trends Cell Biol.*, **9**, 302–309.
58. Lamond, A.I. and Earnshaw, W.C. (1998) Structure and function in the nucleus. *Science*, **280**, 547–553.
59. Spector, D.L. (2003) The dynamics of chromosome organization and gene regulation. *Annu. Rev. Biochem.*, **72**, 573–608.
60. Nayler, O., Schnorrer, F., Stamm, S. and Ullrich, A. (1998) The cellular localization of the murine serine/arginine-rich protein kinase CLK2 is regulated by serine 141 autophosphorylation. *J. Biol. Chem.*, **273**, 34341–34348.
61. Stojdl, D.F. and Bell, J.C. (1999) SR protein kinases: the splice of life. *Biochem. Cell Biol.*, **77**, 293–298.
62. Colwill, K., Feng, L.L., Gish, G.D., Cáceres, J.F., Pawson, T. and Fu, X.D. (1996) SRKP1 and Clk/Sty protein kinases show distinct substrate specificities for serine/arginine-rich splicing factors. *J. Biol. Chem.*, **271**, 24 569–24 575.
63. Hartmann, A.M., Rujescu, D., Giannakouros, T., Nikolakaki, E., Goedert, M., Mandelkow, E.M., Gao, Q.S., Andreadis, A. and Stamm, S. (2001) Regulation of alternative splicing of human tau exon 10 by phosphorylation of splicing factors. *Mol. Cell. Neurosci.*, **18**, 80–90.
64. Shin, C., Feng, Y. and Manley, J.L. (2004) Dephosphorylated SRp38 acts as a splicing repressor in response to heat shock. *Nature*, **427**, 553–558.
65. Baskaran, R., Dahmus, M.E. and Wang, J.Y. (1993) Tyrosine phosphorylation of mammalian RNA polymerase II carboxyl-terminal domain. *Proc. Natl Acad. Sci. USA*, **90**, 11 167–11 171.
66. Welch, P.J. and Wang, J.Y. (1993) A C-terminal protein-binding domain in the retinoblastoma protein regulates nuclear c-Abl tyrosine kinase in the cell cycle. *Cell*, **75**, 779–790.
67. Darnell, J.E., Jr (1997) Phosphotyrosine signaling and the single cell:metazoan boundary. *Proc. Natl Acad. Sci. USA*, **94**, 11 767–11 769.
68. Stamm, S., Zhu, J., Nakai, K., Stoilov, P., Stoss, O. and Zhang, M.Q. (2000) An alternative-exon database and its statistical analysis. *DNA Cell Biol.*, **19**, 739–756.
69. Maniatis, T. and Reed, R. (2002) An extensive network of coupling among gene expression machines. *Nature*, **416**, 499–506.
70. Wu, J.Y. and Maniatis, T. (1993) Specific interactions between proteins implicated in splice site selection and regulated alternative splicing. *Cell*, **75**, 1061–1070.
71. Cazalla, D., Zhu, J., Manche, L., Huber, E., Krainer, A.R. and Caceres, J.F. (2002) Nuclear export and retention signals in the RS domain of SR proteins. *Mol. Cell. Biol.*, **22**, 6871–6882.
72. Xu, Q. and Lee, C. (2003) Discovery of novel splice forms and functional analysis of cancer-specific alternative splicing in human expressed sequences. *Nucl. Acids Res.*, **31**, 5635–5643.
73. Hao, Q.-L., Ferris, D.K., White, G., Heisterkamp, N. and Groffen, J. (1991) Nuclear and cytoplasmic location of the FER tyrosine kinase. *Mol. Cell. Biol.*, **11**, 1180–1183.
74. Derry, J.J., Richard, S., Carvajal, H.V., YE, X., Vasioukhin, V., Cochrane, A.W., Chen, T. and Tyner, A.L. (2000) Sik (BRK) phosphorylates Sam68 in the nucleus and negatively regulates its RNA binding ability. *Mol. Cell. Biol.*, **20**, 6114–6126.
75. Zhang, J., Berenstein, E.H., Evans, R.L. and Siraganian, R.P. (1996) Transfection of Syk protein tyrosine kinase reconstitutes high affinity IgE receptor-mediated degranulation in a Syk-negative variant of rat basophilic leukemia RBL-2H3 cells. *J. Exp. Med.*, **184**, 71–79.
76. König, H., Ponta, H. and Herrlich, P. (1998) Coupling of signal transduction to alternative pre-mRNA splicing by a composite splice regulator. *EMBO J.*, **17**, 2904–2913.
77. Jumaa, H. and Nielsen, P.J. (1997) The splicing factor SRp20 modifies splicing of its own mRNA and ASF/SF2 antagonizes this regulation. *EMBO J.*, **16**, 5077–5085.